Hensin Remodels the Apical Cytoskeleton and Induces Columnarization of Intercalated Epithelial Cells: Processes that Resemble Terminal Differentiation

S. Vijayakumar, Jiro Takito, Chinami Hikita, and Qais Al-Awqati

Department of Medicine and Department of Physiology, College of Physicians and Surgeons of Columbia University, New York 10032

Abstract. Intercalated epithelial cells exist in a spectrum of phenotypes; at one extreme, β cells secrete HCO_3 by an apical Cl/HCO_3 exchanger and a basolateral H^+ ATPase. When an immortalized β cell line is seeded at high density it deposits in its extracellular matrix (ECM) a new protein, hensin, which can reverse the polarity of several proteins including the Cl/HCO_3 exchanger (an alternately spliced form of band 3) and the proton translocating ATPase. When seeded at low density and allowed to form monolayers these polarized epithelial cells maintain the original distribution of these two proteins. Although these cells synthesize and secrete hensin, it is not retained in the ECM, but rather, hensin is present in a large number of intracellular vesicles. The apical cytoplasm of low density cells is devoid of actin, villin, and cytokeratin19. Scanning electron microscopy shows that these cells have sparse microvilli, whereas high density cells have exuberant apical surface infolding and microvilli. The apical cytoplasm of high density cells contains high levels of actin, cytokeratin19, and villin. The cell shape of these two phenotypes is different with high density cells being tall with a small cross-sectional area, whereas low density cells are low and flat. This columnarization and the remodeling of the apical cytoplasm is hensin-dependent; it can be induced by seeding low density cells on filters conditioned by high density cells and prevented by an antibody to hensin. The changes in cell shape and apical cytoskeleton are reminiscent of the processes that occur in terminal differentiation of the intestine and other epithelia. Hensin is highly expressed in the intestine and prostate (two organs where there is a continuous process of differentiation). The expression of hensin in the less differentiated crypt cells of the intestine and the basal cells of the prostate is similar to that of low density cells; i.e., abundant intracellular vesicles but no localization in the ECM. On the other hand, as in high density cells hensin is located exclusively in the ECM of the terminally differentiated absorptive villus cells and the prostatic luminal cell. These studies suggest that hensin is a critical new molecule in the terminal differentiation of intercalated cell and perhaps other epithelial cells.

Key words: epithelial polarity • terminal differentiation • intercalated cells • cell shape • hensin

EPITHELIA, the first differentiated cells to develop in the embryo, exhibit polarized plasma membrane domains and cytoplasm, with the nuclei occupying the basal half of the cell (Eaton and Simons, 1995; Drubin and Nelson, 1996). Epithelia are attached to each other by several types of junctions and rest on an extracellular matrix (ECM)[1] that they largely synthesize. The fact that epithelial cells in different organs share all these characteristics, yet are recognizably different from each other, implies that development and differentiation of epithelia proceeds in at least two steps: conversion of a nonepithelial cell to a proto-epithelium, and terminal differentiation. Proto-epithelial cells exhibit the fundamental properties of epithelia, but are still able to divide and migrate. Terminally differentiated epithelia, while losing motile and proliferative behavior, acquire specific features such as: brush borders, specialized organelles (e.g., storage granules), characteristic cell shape (e.g., columnarization), and other tissue specific properties. Terminal differentiation continues to occur in adult animals in the intestine, skin, prostate, and other organs. Recent studies in many organisms have shown that interruption of such differentiation programs leads to unbridled growth leading to, or contributing to, the development of cancer.

Address correspondence to Qais Al-Awqati, Department of Medicine and Physiology, College of Physicians and Surgeons of Columbia University, 630 West 168th Street, New York, NY 10032. Tel.: 212-305-3512. Fax: 212-305-3475. E-mail: qa1@columbia.edu

1. *Abbreviations used in this paper:* CUB, complement subcomponents Clr/Cls, Uegf, Bmp1; ECM, extracellular matrix; FAK, focal adhesion kinase; kAE1, kidney form of the anion exchanger1; SRCR, scavenger receptor cysteine rich; ZP, zona pellucida.

We were led to issues of terminal differentiation while studying the targeting of ion transport proteins in a kidney epithelial cell line derived from intercalated cells. These cells are specialized for transepithelial acid transport, mediated by a polarized H^+ ATPase and a Cl^-/HCO_3^- exchanger, which is an alternately spliced form of the red cell band 3 (kAE1, kidney anion exchanger1). In situ, they exist in a spectrum of forms with two extremes: one secretes acid by an apical H^+ ATPase and a basolateral anion exchanger (the α-form), whereas the other (β) secretes HCO_3^- by an apical exchanger and a basolateral ATPase (for review see Schuster, 1993; Al-Awqati et al., 1998). H^+ ATPase (α-form) is packaged in vesicles that continuously recycle by endocytosis and exocytosis at the apical membrane in a process regulated by cell pH and calcium (Gluck et al., 1982; Cannon et al., 1985). Remarkably, the β cells had no apical endocytosis, suggesting that the apical cytoplasm of the two cell types were fundamentally different, as was clear in transmission electron micrographs of these cells.

We (and others) noticed that feeding animals an acid diet reversed the ion transport properties of the collecting tubule of the kidney from HCO_3^- secretion to HCO_3^- absorption (i.e., H^+ secretion). We provided initial physiological evidence that this reversal happened because β cells converted to α cells (Schwartz et al., 1985). To study the biochemical pathway, we generated an immortalized β cell line that had an apical kAE1 and a basolateral H^+ ATPase (Edwards et al., 1992). When these clonally derived cells were seeded at subconfluent density and examined (after they formed an epithelium), they secreted HCO_3^- to the lumen and had apical kAE1 and basolateral H^+ ATPase (van Adelsberg et al., 1993). Seeding the cells at confluent densities resulted in their conversion to the following: an α phenotype, with transepithelial HCO_3^- absorption; an apical H^+ ATPase; a basolateral kAE1; and vigorous apical endocytosis. The high density cells secreted a new protein and localized it to their ECM (van Adelsberg et al., 1994). Using an assay for apical endocytosis, we purified this protein from high density ECM. The purified protein was able to reverse the phenotype of these cells. This new protein, which we termed hensin (for change in body in Japanese) is expressed in epithelial cells and the brain. In the kidney it is restricted to the collecting tubule (Takito et al., 1996). We show here that hensin induces a reorganization of the apical membrane and its associated cytoskeleton with the expression of villin and cytokeratin19, two proteins that are necessary for the formation of microvilli. Further, these changes lead to columnarization of the intercalated cells. All of these changes are similar to what occurs in terminal differentiation of other epithelia. Therefore, we suggest that the change in phenotype is a process of terminal differentiation and that hensin is a critical new molecule in this pathway.

Materials and Methods

Cell Culture

Stock cultures of clone C of β-intercalated cells established from rabbit kidney cortex were maintained as described (van Adelsberg et al., 1993, 1994). The cells were trypsinized and seeded on polycarbonate filters (pore size, 0.4 μm; Costar Corp.) at a density of 2×10^4 cells/cm^2 (low density), or 10^6 cells/cm^2 (high density), and transferred to 40°C to inactivate the T antigen. At temperatures between 37° and 40°C, no positive staining of the T antigen was observed by immunofluorescence or immunoblot analysis.

Pulse Labeling and Immunoprecipitation of Hensin

High or low density cells on polycarbonate filters were pulse-labeled with 100 μCi/ml of [^{35}S]methionine added to both apical and basal media (^{35}S-protein labeling mix; DuPont-NEN) for 5 min at 40°C at various time intervals. Cells were lysed in buffer A (1% SDS, 1 mM EDTA, 1% Triton X-100, 10 mM Tris-HCl, pH 8.0) and boiled for 3 min. Insoluble materials were removed by a brief centrifugation (14,000 *g* for 5 min at room temperature) and the protein concentration of the supernatants was determined by the Bradford reagent (Bio-Rad Laboratories). An equal amount of protein was taken from each sample, diluted 10-fold with 10 mM Tris-HCl, pH 8.0, and used for immunoprecipitation.

Clone C cells seeded at high or low density were cultured for 5 d and labeled with ^{35}S-protein labeling mix added to both apical and basal media for 12 h. Apical and basolateral media were collected separately and centrifuged at 5,000 *g* for 5 min at 4°C. The supernatants were mixed with 1/10 vol of buffer A and analyzed by immunoprecipitation.

Samples from the pulse labeling experiments and secretion studies were incubated with 1:500 dilution of guinea pig anti-hensin antiserum at 4°C for 1 h. Immunoprecipitates were collected by mixing the samples with protein A–Sepharose CL-4B (Pharmacia Biotech, Inc.) at 4°C for 1 h. The beads were washed with a buffer containing 0.1% SDS, 0.1 mM EDTA, 0.1% Triton X-100, and 10 mM Tris-HCl, pH 8.0. Immunoprecipitated protein samples were extracted from the beads by boiling them in SDS-PAGE sample buffer for 3 min. Thus, samples extracted were subjected to SDS gel electrophoresis in 7.5% gel. Gels were fixed with 10% acetic acid, 10% methanol, soaked in solution (Amplify; Amersham Pharmacia Biotech), dried, and exposed to X-ray film (Kodax X-OMAT) at −80°C. Films were developed and analyzed using a densitometer (model 300A; Molecular Dynamics, Inc.).

Immunoblot Analysis

Intermediate filament fraction was prepared from confluent monolayer cultures of both low and high density cells with a modified procedure of previously published protocols (Achtstaeter et al., 1986; Stasiak et al., 1989). In brief, monolayers were lysed with a solution containing 10 mM Tris-HCl, pH 7.6, 140 mM NaCl, 5 mM EDTA, 15 mM β-mercaptoethanol, 1 mM PMSF, and 1% Triton X-100 for 3–5 min at 4°C. The lysis buffer was aspirated and the monolayer was extracted with a high salt buffer (10 mM Tris-HCl, pH 7.6, 140 mM NaCl, 1.5 M KCl, 5 mM EDTA, 0.5% (wt/vol) Triton X-100, 15 mM β-mercaptoethanol, and 1 mM PMSF, at 4°C for 1 h. The extract was centrifuged for 30 min at 3,000 *g* (4°C) and the pellet was washed with buffer (10 mM Tris-HCl, pH 7.6, 140 mM NaCl, and 5 mM EDTA). The final pellet was dissolved in SDS-PAGE buffer, the sample was electrophoresed in a 10% SDS-PAGE gel, transferred to a nitrocellulose membrane, and probed with anticytokeratin19 antibody (MAB1675). These samples were prepared from an equal number of cells.

Immunocytochemistry

The immortalized intercalated cells (clone C) were plated at high or low density and cultured for 1–2 wk at 40°C on Transwell filters, depending on the experiment. The following procedures were performed at room temperature: cells were fixed in 4% paraformaldehyde for 10 min, blocked, and permeabilized in a solution of 3% BSA and 0.075% saponin in PBS, pH 7.4, for 1 h. The Transwell filters were incubated in primary antibodies diluted 1:100 in the PBS/BSA/saponin solution for 1–2 h. The following primary antibodies were used: mouse mAb to E-cadherin (MAB 1996), fodrin (MAB 1622), cytokeratin19 (MAB 1675), villin (MAB 1671) and rat anti-ZO1 antibody (MAB 1520) (all from Chemicon International, Inc.) and anti–β-tubulin antibody (Boehringer Mannheim GmbH). Fluorescein- or rhodamine-labeled goat anti–mouse IgG and rhodamine-labeled donkey anti–rat IgG (Jackson ImmunoResearch Laboratories) were used as secondary antibodies. For F-actin staining, the filters were incubated with 300–600 U of rhodamine-phalloidin (R-415) (Molecular Probes, Inc.).

Stained monolayers were mounted on glass slides with 90% glycerol in PBS with 0.1% phenylene diamine and viewed by an Axiovert 100 laser-

scanning confocal microscope (model LSM 410; Carl Zeiss). Excitation was accomplished with an argon-krypton laser producing lines at 488, 568, or 647 nm. Rhodamine- and Cy3-labeled samples were viewed with the 568-nm channel (red), whereas the fluorescein–Hoechst 33342-labeled samples were viewed with the 488-nm channel (green). In the case of triple labeling with Hoechst/hensin and collagen type IV, the Cy5-conjugated collagen type IV antigens were visualized with the deep red 645-nm channel. The images were collected at 1 μm thickness optical sections and analyzed by the Zeiss LSM-PC software. The final images were processed with Adobe Photoshop software.

Immunocytochemistry with Anti–hensin Antibody

Guinea pig anti–hensin antibodies were obtained as described earlier (Takito et al., 1996). A fusion protein containing scavenger receptor cysteine rich (SRCR) domains 5 and 6 of hensin (Takito et al., 1996) was used to generate these antibodies. The immortalized intercalated cells (clone C) were plated at high or low density and cultured for 1–2 wk at 40°C on Transwell filters depending on the experiment. In the studies aimed at determining the extracellular accessibility of hensin, the filters were first incubated with 10–20 μg/ml of Hoechst 33342 dye (Molecular Probes, Inc.). After extensive washing with PBS, cells were incubated in 1:50 dilution of guinea pig anti-hensin antibody solution in PBS alone, or with 1:100 dilution of the mouse anti–collagen type IV mAb (MAB 1910; Chemicon International, Inc.) overnight at 4°C. The filters were washed with PBS and incubated with rhodamine–Cy3 conjugated anti–guinea pig IgG (Jackson ImmunoResearch Laboratories, Inc.) alone, or with Cy5 conjugated anti–mouse IgG (for collagen IV triple label experiment) for 1 h at room temperature. The filters were washed, fixed for 30 s–1 min with ice-cold methanol, washed extensively with PBS, and mounted and analyzed with confocal microscopy as described before. Control experiments were performed to test whether prolonged incubation at 4°C resulted in cellular permeabilization. When the guinea pig anti-hensin antibody and anti–β-tubulin mAb were incubated together under the same conditions, we found no specific staining for tubulin, whereby indicating that the cells remained impermeable to these molecules.

For studies involving the determination of cellular localization of hensin, the confluent monolayers of high or low density clone C cells were first incubated in Hoechst 33342 at 10–20 μg/ml for 1 h at room temperature, washed with PBS, and fixed with ice-cold methanol for 1 min. After extensive washing with PBS, cells were permeabilized by incubating with a solution of PBS/BSA/saponin (as described above) and incubated further with guinea pig anti-hensin antibody, followed by rhodamine–Cy3 conjugated anti–guinea pig IgG.

Immunohistochemistry of Rabbit Tissues

Prostate glands and intestinal tissues obtained from male New Zealand white rabbits (Hare Marland) were embedded and frozen in tissue-tek OCT compound (Miles Laboratories) until cut into 5-μm cryostat sections. The sections were fixed in ice-cold methanol for 8 min, washed extensively with PBS, and blocked with 10% FCS and 1% donkey serum (Jackson ImmunoResearch Laboratories, Inc.) in PBS for 30 min. The sections were incubated with guinea pig anti–hensin antibody (Takito et al., 1996), diluted 1:100 in PBS at room temperature for 2 h and incubated with rhodamine-conjugated donkey anti–mouse IgG. The prostate sections were further incubated with FITC-conjugated monoclonal anti-cytokeratin7 (F-3772; Sigma Chemical Co.) diluted 1:25 in PBS. Finally, sections were extensively washed and mounted for analysis under a confocal microscope.

Analysis of the Shape and Height of Clone C Cells

All analyses of cell size and height were performed with Microsoft Windows® based version of the Zeiss 410 laser scanning microscope software (Carl Zeiss GmbH). The stepper motor and the image analysis software use the internal calibration method for this microscope. All 1-μm sections of a particular field from a sample of phalloidin-stained low or high density cells were projected on the screen together with maximum overlap and all other default settings of the Zeiss LSM-PC software. For size measurements, individual cell boundaries were delineated using a mouse-driven marker (via the Mark Area subfunction of the Area Measure function of this software) and the area obtained in μm^2 is recorded. The area of 10–15 individual cells of each sample were recorded and were analyzed statistically with the program Corel Quattro Pro.

For measuring the height of the cells, the xz-section of the sequence of images from each specific sample is used. The two "posit" (position marker) cursors are placed on the same x-coordinate of the xz-section. However, one "posit" cursor is placed on the y-coordinate, corresponding to the first observed apical stain above the nucleus, and the other is placed on the last observed basal stain below the nucleus. The distance measurement function of the Zeiss LSM-PC software is invoked to measure the height. Again, 10–15 individual measurements were recorded for each sample and were analyzed statistically using Corel Quattro Pro. For all these measurements, the phalloidin- or phallodin–Hoechst 33342-stained samples were used to ensure the uniformity of the measurements.

Scanning Electron Microscopy

Filters were washed in PBS and fixed with 2.5% glutaraldehyde in 100 mM phosphate buffer. The filters were postfixed for 1 h in 1% osmium tetroxide/1.5% potassium ferricyanide and dehydrated through a graded ethanol series: 50, 70, 85, 95, 100, 100, 100% for 10 min at each concentration. Afterwards, cells underwent critical point drying using CO_2 in an Omar SPC-1500 critical point dryer. The filters were cut from their holders and mounted on copper specimen supports, sputter-coated with ~11 nm of Au-Pd in a sputtering unit (Pelco 91000; Ted Pella Inc.), and viewed at 20 kV in an electron microscope (JEOL 100 CX-II; JEOL USA, Inc.) equipped with an ASID scanning unit and images were recorded on Polaroid Type 55 positive/negative film.

Antibody Blocking Experiments

Guinea pig anti–hensin antisera (Takito et al., 1996) were diluted 1:100 in the culture medium. Anti-laminin B2 mAb obtained as hybridoma supernatant D18 from the Developmental Studies Hybridoma Bank (University of Iowa, Iowa City, IA) was diluted in the culture medium to a final concentration of 30 μg/ml and mouse anti–human collagen type IV mAb was diluted to a final concentration of 60 μg/ml in the culture medium. Confluent monolayers of clone C cells grown at 32°C were trypsinized and centrifuged. The cell pellet was resuspended in the appropriate antibody-containing culture medium and plated at high density (10^6 cells/cm^2). Antibody-containing culture medium was replaced daily for 5 d and the cells were processed for immunocytochemistry as described above.

Experiments on Low Density Cells Grown on High Density Matrix and Various ECM Components

Hensin containing ECM-coated filters were obtained through the following procedure: (a) High density cells cultured on Transwell filters for 1 wk were extracted with 1% Triton X-100, 1 mM calcium chloride for 1 h at 4°C on a rotary shaker. (b) Cell extracts were removed and filters were scraped in this solution with a cell scraper to remove loosely attached materials. (c) Filters were washed thoroughly with the same solution for another hour at 4°C followed by three washes with the culture medium. (d) The filters were left overnight in the culture medium on a 4°C-rotary shaker and clone cells were seeded on such filters and cultured as usual. Murine laminin-coated Transwell filters, human fibronectin coated Transwell filters, and Matrigel basement membrane matrix- (from Engelbreth-Holm-Swarm Mouse Sarcoma) coated cell culture inserts were obtained from Becton Dickinson Labware (models: 40441, 40615, 40443, respectively). The laminin- and fibronectin-coated filters were rehydrated by incubation with culture medium for 30 min at room temperature before seeding the cells. In the case of Matrigel-coated filters, the filters were thawed overnight on a level surface at 4°C and the Matrigel solution from one Transwell filter was spread on two Transwell filters (model 3412; Costar Corp.) before rehydration and seeding. This was necessary as the thick gelatinous layer of matrigel present on the precoated filters (model 40443; Becton Dickinson Labware) prevented the immunohistochemical analysis of the cells cultured on them.

Results

Hensin Is Localized in the Extracellular Space of High Density but Not Low Density Cells

Initial studies showed that high density ECM contained a new protein (hensin) that induced the reversal of polarity,

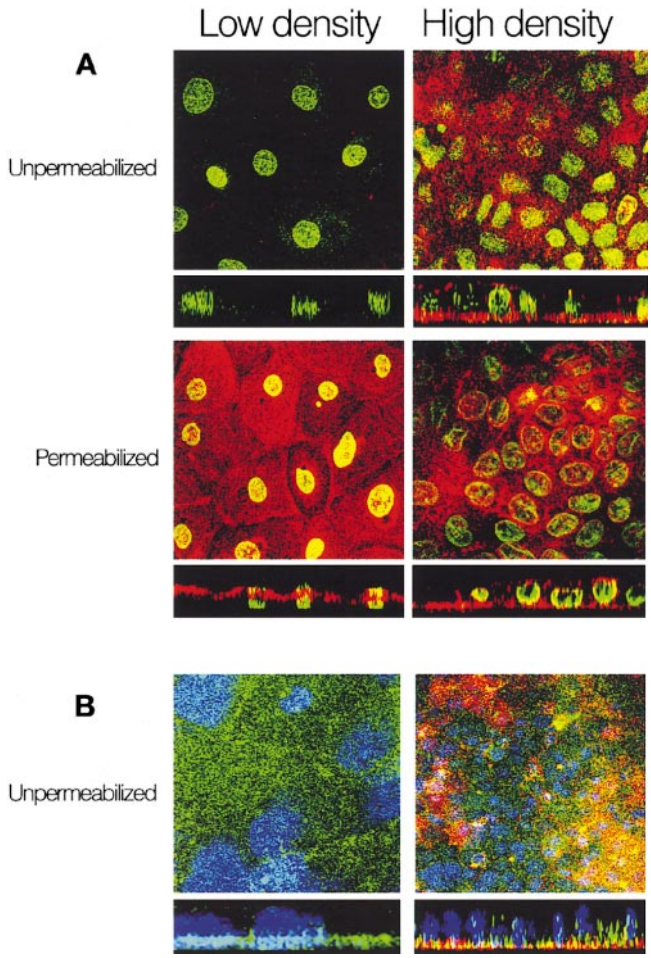

Figure 1. Distribution of hensin in intercalated cells seeded at high and low densities. (A) Intercalated cells seeded at low density (left) and high density (right) were either unpermeabilized, or fixed with methanol and permeabilized with saponin, and stained with anti-hensin antibodies and a nuclear stain (Hoechst 33342). As can be seen, hensin is accessible to the anti-hensin antibodies only in the unpermeabilized high density cells, not in the low density cells. The apical cytoplasmic localization of hensin in low density cells and the extracellular localization of hensin in high density cells can be seen in two pictures (bottom) of permeabilized cells. (B) Colocalization of hensin with collagen type IV in high density cells. Unpermeabilized high and low density intercalated cells were stained with guinea pig anti-hensin polyclonal antibodies and mouse anti–collagen type IV mAb along with a nuclear stain as described in Materials and Methods. Low density cells had no extracellular deposits of hensin (red), although collagen IV (green) was visible in the basement membrane. However in high density cells both hensin and collagen IV were extracellular and colocalized (yellow). In these pictures the nuclear staining is shown in blue.

but the low density matrix did not. We generated antibodies to a hensin fusion protein containing SRCR domains 6 and 7 (Takito et al., 1996) that were used for immunoprecipitation and immunocytochemistry. Fig. 1 shows the results of immunocytochemistry using confocal microscopy. Low density monolayers incubated with the anti-hensin antibodies, in the absence of detergents, showed no hensin staining. Therefore, the absence of hensin in the extracellular space of these cells demonstrates and confirms our previous biochemical results (van Adelsberg et al., 1994; Takito et al., 1996). Low density cells like other epithelia, secrete collagen IV into their ECM, was found to be accessible to anti–collagen IV antibodies in the absence of detergents (Fig. 1 B).

To examine whether hensin was present in the extracellular space of high density cells, we exposed the cells to anti-hensin antibody in the absence of detergents. Hensin was found to be accessible to the antibody (Fig. 1 A, unpermeabilized cells) and its distribution was similar to that of collagen IV (Fig. 1 B). Note that both hensin and collagen IV were deposited on the filters as shown by the colocalization in the xy confocal planes (Fig. 1 B). These results demonstrate that hensin localizes to the basal and lateral regions of the extracellular space of high, but not low density cells and overlaps in distribution, at least partially, with a bona fide ECM protein. Surprisingly, when the cells were permeabilized by saponin, we found that even low density cells contained a large number of hensin-containing intracellular vesicles located diffusely throughout the cell, including the apical half. On the other hand, the high density cells contained few intracellular vesicles staining for hensin. This difference in distribution started at the earliest time examined (3 h of plating) and reached the final distribution within a few days.

To examine the initial rate of hensin synthesis, cells were plated at high or low density on nucleopore filters and labeled with a short pulse of [^{35}S]methionine at various times after seeding. We found that low density cells, reproducibly, had higher levels of synthesis (Fig. 2 A). To examine the secretion of hensin, the cells were labeled for 12 h with [^{35}S]methionine and the apical and basolateral media were collected and immunoprecipitated. Both phenotypes secreted hensin in a polarized manner to the basolateral medium (Fig. 2 B).

The Apical Cytoskeleton in High and Low Density Cells

The induction of apical endocytosis is the most dramatic and reproducible effect in the conversion of low density phenotype to that of high density. Apical endocytosis, or its lack, clearly reflects large alterations in the apical cytoskeleton. We examined components of this cytoskeleton and found dramatic differences as a function of seeding density (see Figs. 3–5). F-actin, in low density cells, was located underneath the basal and lateral membranes but there was only a faint, if any, staining under the apical membranes. High density cells had dense subapical actin network (in addition to the basolateral network). There were more stress fibers in the basal region of low density phenotype, perhaps suggesting that these cells might be less well-differentiated than the high density cells (Fig. 4, F-actin). Remarkably, cytokeratins were also quite different. Cytokeratin19, recently implicated in the organization of the terminal web of intestinal epithelial cells (Salas et al., 1997), was largely absent from low density cells but was abundant in high density cells (Fig. 4, Cytokeratin-19). More significantly, cytokeratin19 was located mostly in the subapical region of the cells. These studies suggest that the terminal web, an actin–cytokeratin mesh critical for the

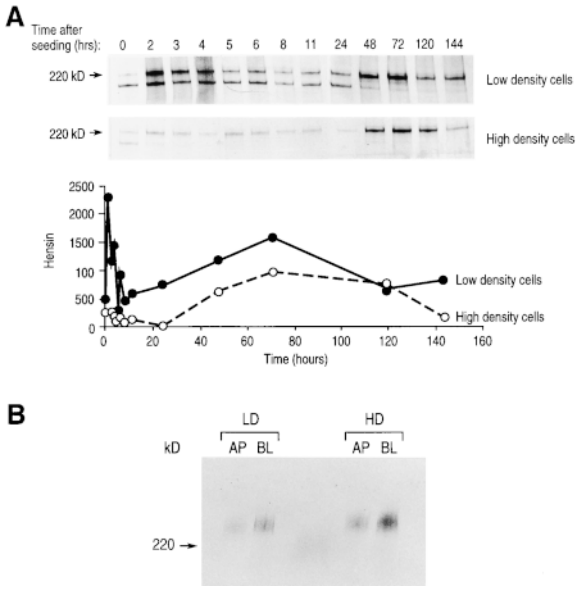

Figure 2. Biochemical characterization of the synthesis and secretion of hensin. (A) Low density and high density cells were pulse-labeled with [^{35}S]methionine for 5 min at the indicated time intervals after seeding and analyzed by immunoprecipitation as described in Materials and Methods. Densitometric analysis of the results is shown below. (B) Intercalated cells seeded at low or high density, cultured for 5 d, and labeled with [^{35}S]methionine for 12 h. Hensin was immunoprecipitated from the apical and basolateral media. Both low and high density cells secreted hensin in a polarized manner to the basolateral medium.

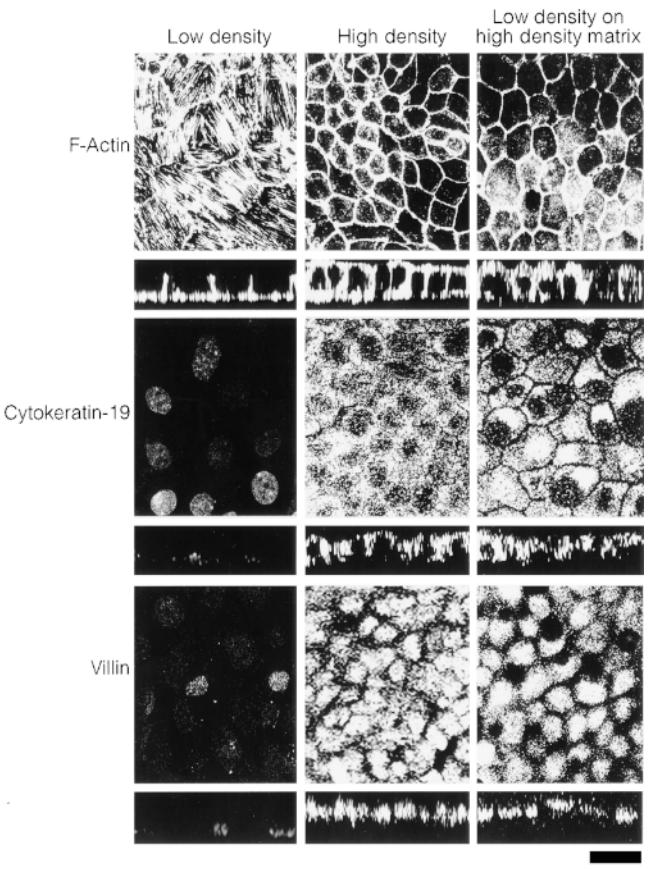

Figure 4. Distribution of F-actin, cytokeratin19, and villin in intercalated cells. Intercalated cells seeded at low (left) or high densities (middle) and at low density on a high density ECM (right). They were analyzed by immunocytochemistry 1 wk after seeding as described in Materials and Methods. Actin was visualized by staining with rhodamine-phalloidin, whereas villin and cytokeratin19 were stained with mAb. In the xz sections, the bottom of each image represents the level of the filter. Bar, 25 μm.

formation of microvilli, was substantially different in the two phenotypes. When the microfilament fraction of low density cells was extracted and subjected to immunoblot analysis, no cytokeratin19 was found, whereas that of high density cells was quite enriched in this protein. This result suggests that high density cells can synthesize this protein (Fig. 5).

Next, we examined the distribution of villin, the most critical actin-binding protein for microvillar structure (Friedrich et al., 1989), and found that its expression in low density cells was barely detectable; when seen it was expressed in a faint cytoplasmic pattern. In high density cells, villin was highly expressed and located entirely in the apical region of the cell in a manner suggestive of incorporation in microvilli (Figs. 3 and 4, Villin). These studies are reminiscent of the development of the apical cytoskeleton in the intestine; the epithelial cells of the crypt (including stem cells) have essentially no villin or subapical cytokeratin but as they migrate up the villus to become terminally differentiated, they start expressing villin and cytokeratins and develop a thick brush border (Louvard et al., 1992). This complex pattern of new gene expression suggest activation of a differentiation pathway.

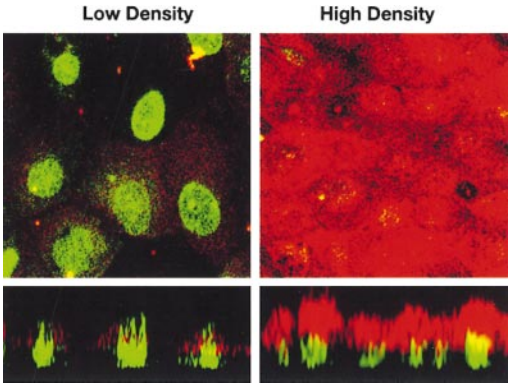

Figure 3. Distribution of villin in low density and high density phenotypes. Low and high density phenotype intercalated cells were stained with anti-villin mAb (red) and the nuclear stain Hoechst 33342 (green).

Although the above observations might suggest that low density cells are undifferentiated, in fact, these cells are bona fide epithelial cells. They show polarized distributions of proteins (van Adelsberg et al., 1993, 1994), lipids (van't Hof et al., 1997), and polarized secretion of hensin (Fig. 2). They are also capable of steady state transepithelial transport of HCO_3^-, which would not be possible with-

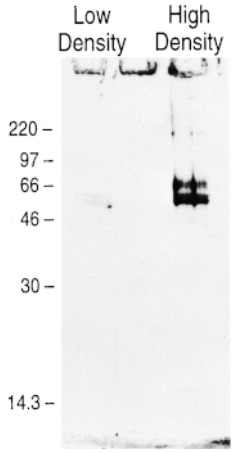

Figure 5. Immunoblot analysis of cytokeratin19 in the microfilament fraction of low and high density intercalated cells. Intermediate filaments were extracted from equal number of cells of both low and high density phenotype intercalated cells as described in Materials and Methods and probed with a mAb to cytokeratin19.

out polarized distribution of transport proteins and sufficiently impermeant intercellular junctions (van Adelsberg et al., 1993, 1994). Further, low density cells have all of the following: well-formed tight junctions (Fig. 6, ZO-1); adherent junctions (Fig. 6, E-Cadherin); a polarized cytoskeleton, where F-actin was present in lateral and basal surfaces (Fig. 4, F-actin); and fodrin in the lateral membranes (Fig. 6, Fodrin). There was also no significant difference in the distribution of paxillin and focal adhesion kinase (FAK; not shown) in the two phenotypes.

Intercalated cells in situ do not exhibit brush borders, but scanning electron microscopy showed that their apical cell membranes have impressive specializations: β-intercalated cells have apical microvilli whereas α-intercalated cells have apical folds, termed microplicae (Hagege and Richet, 1970; LeFurgey and Tisher, 1979). The latter are broad apical ridges that are readily observed in scanning electron micrographs of mammalian kidney and their homologous epithelia in amphibia and reptiles. We performed scanning electron microscopy on low and high density cells and found that low density cells had few apical microvilli scattered over the apical surface that did not change with length of time in culture. Fig. 7 shows low density cells after 1 wk in culture. After 1 wk in culture at high density, the number of well-formed microvilli was much higher and they appeared to be taller and thicker than those in low density cells. In addition, a substantial fraction of the cells had clearly established microplicae (Fig. 7). After 2 wk in culture, all high density cells had microplicae of different dimensions and very large microvilli (Fig. 7). These results demonstrate that the transition of low to high density phenotypes represents a fundamental change in the properties of the apical cytoskeleton and by analogy with other epithelia, we suggest that it represents a terminal differentiation phenomenon.

High Seeding Density Induces Columnarization

Differentiation of epithelial cells is associated with changes in cell shape. Indeed, it has been suggested that a change in shape itself might induce terminal differentiation (Chen et al., 1997). Protoepithelial cells are flat with a large apical surface area, whereas terminally differentiated epithelia are taller and more tightly packed. This process

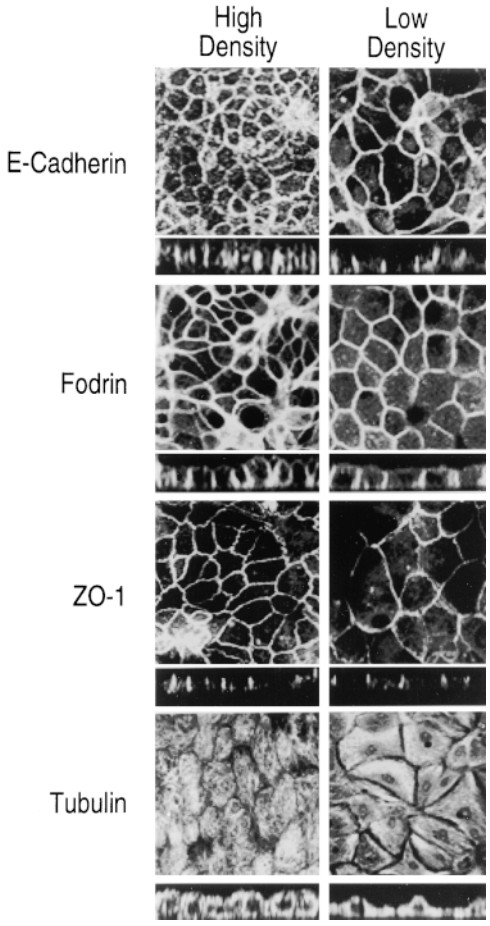

Figure 6. Distribution of E-cadherin, fodrin, ZO-1, and tubulin in intercalated cells seeded at low and high seeding densities. Intercalated cells were seeded at the indicated densities and cultured for 1 wk. The cells were fixed and stained with mAb to E-cadherin, fodrin, ZO-1, and tubulin. The xz sections of both phenotypes reveal the characteristic basolateral localizations for E-cadherin and fodrin and the apical tight junction localization for ZO-1. The tubulin network is similar in both phenotypes.

of columnarization is frequently seen during development (Bard, 1990). Examination of Figs. 3, 4, 6, and 7, shows that low density cells are thin and have a large cross-sectional area whereas high density cells are columnar, tall

Table I. Measurement of Cross-sectional Area and Cell Height

	Height	Cross-sectional area
	μm	μm^2
Low density	4.75 ± 0.2	841 ± 83
High density	8.73 ± 0.3	185 ± 12
High density + anti-hensin Ab	4.61 ± 0.2	385 ± 23
High density + anti–collagen IV Ab	9.06 ± 0.2	205 ± 18
High density + anti–laminin Ab	8.61 ± 0.3	225 ± 15
Low on high density matrix	9.06 ± 0.2	233 ± 22
Low density on laminin	5.53 ± 0.2	1,867 ± 145
Low density on fibronectin	5.32 ± 0.3	2,234 ± 162
Low density on matrigel	5.77 ± 0.3	2,343 ± 143

Results obtained from confocal images of phalloidin stained cells as described in Materials and Methods. For each experiment, 11 cells were analyzed and the results are expressed as means ± SEM.

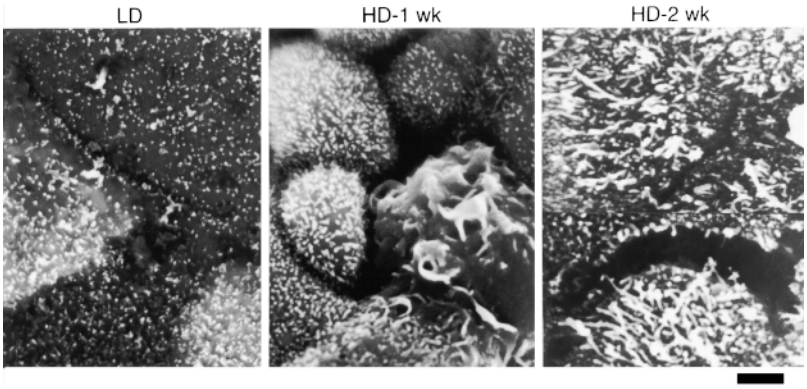

Figure 7. Scanning electron micrographs of the apical surface of intercalated cells seeded at low (LD) and high (HD) densities. Low density intercalated cell images are shown after 1 wk in culture. When cultured for an additional week they showed no change. Bars: (left and middle) 7 μm; (right) 5 μm.

with smaller cross-sectional area. Quantitative analysis of the confocal images is shown in Table I. On average, low density cells have a cross-sectional area of 841 ± 83 μm^2 whereas that of high density cells was 185 ± 12 μm^2. The height of low density cells was 4.75 ± 0.2 μm, but that of high density cells was 8.73 ± 0.2 μm (mean ± SEM, $P <$ 0.01, Table I).

Hensin Mediates the Remodeling of the Apical Cytoskeleton and Columnarization

To examine whether hensin mediates columnarization and cytoskeletal changes, we seeded cells at low density on filters that were coated with a high density matrix. These conditioned filters were prepared by seeding cells at high density for 1 wk, solubilizing with Triton X-100, and discarding remnants. Fresh cells were seeded at low density. Within 1 wk of plating, these low density cells were instructed by the high density matrix to become columnar epithelial cells resembling high density cells. The cell height was 9.06 μm ± 0.2 (Table I) and the cross-sectional area became 233 μm^2 ± 22. High density matrix was also able to change the actin, villin, and cytokeratin19 distribution in these low density cells so that it resembled that of high density cells (Fig. 4). Cells plated at low density on filters pretreated with pure ECM proteins, such as fibronectin and laminin, failed to induce the appearance of subapical actin or change their shape (Fig. 8, Table I). When the cells were plated on matrigel, a complex mixture of many extracellular proteins (produced by the epithelial EHS murine tumor cell line), there was no columnarization or the appearance of subapical actin (Fig. 8, Table I). Hence, the conversion of low density phenotype to a high density one, was not merely due to the presence of the known ECM proteins.

Hensin was purified using an assay that reflects reorganization of the apical cytoplasm, i.e., apical endocytosis (van Adelsberg et al., 1994). Further, in high density cells, antibodies to hensin inhibited the development of apical endocytosis while preimmune sera were ineffective (Takito et al., 1996). In similar experiments, we seeded cells at high density in the presence of anti-hensin antibodies and examined for the development of subapical actin cytoskeleton. Fig. 9 shows that very little actin localized to the apical cytoplasm and the basal surface of these high density cells now contained many stress fibers similar to the basal surface of low density cells. The anti-hensin antibodies also reversed the change in cell shape that was induced by high density plating. When cells were seeded at high density in the presence of anti-hensin antibodies, their height collapsed to that of low density cells, decreasing to 4.6 ± 0.2 μm and the cross-sectional area increased to 385 ± 23 μm^2 (Table I, $n = 11$, $P < 0.01$). Treatment of high density cells with nonimmune guinea pig serum (at the same concentration), or with antibodies to laminin or collagen IV did not prevent the appearance of the subapical actin network, nor did they inhibit the columnarization (Fig. 9, Table I). These results demonstrate that when intercalated

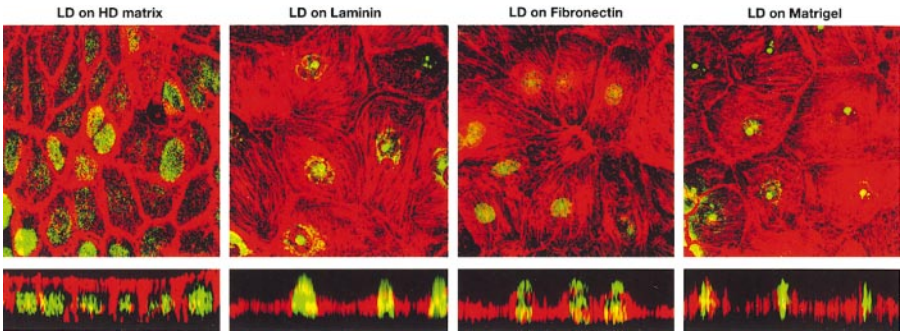

Figure 8. Induction of apical cytoskeleton in low density cells grown on filters conditioned by hensin or other matrices. Intercalated cells were seeded at low density on Transwell filters conditioned with the ECM component of the high density cells or on Transwell filters treated with laminin, fibronectin, or matrigel as described in Materials and Methods. The cells were stained with Hoechst 33322 (green) and rhodamine-phalloidin (red). The top panels represent the projected image of all (8–10 sections of 1 μm each) and the bottom panels represent the xz sections.

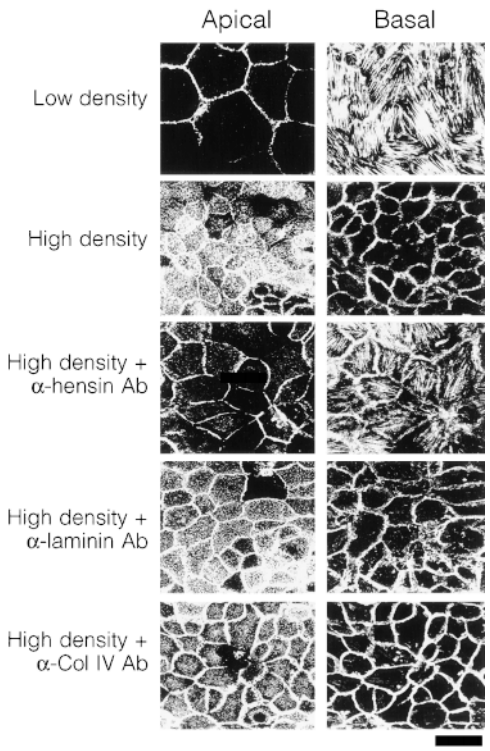

Figure 9. Anti-hensin antibodies prevent the reorganization of the actin cytoskeleton in high density cells. High density intercalated cells were seeded in the presence or absence of polyclonal anti-hensin serum (1:100), anti–laminin mAb (30 μg/ml), and anti–collagen IV mAb (60 μg/ml). The culture media with and without the antibodies were replaced daily. Staining with rhodamine-phalloidin was performed 5 d after seeding. A 2-μm thick apical section (left) is shown. A basolateral optical section (right) of the same thickness is shown. Bar, 25 μm.

cells are seeded at high density, it is hensin that mediates the reorganization of the actin cytoskeleton and columnarization rather than other ECM proteins.

Distribution of Hensin In Two Differentiating Epithelia

One of the best described terminal differentiation events is the intestinal stem cell ascends to the villus tip to become the terminally differentiated absorptive enterocyte (Louvard et al., 1992; Simon and Gordon, 1995). Because the highest level of expression of hensin is in the intestine (Takito et al., 1996), we examined the distribution of hensin in intestinal epithelia. Remarkably, hensin was present in the crypt, largely in a diffuse intracellular pattern that was mostly in the apical half of the cell with no staining of the ECM, (Fig. 10 A) similar to the staining pattern of permeabilized low density cells shown in Fig. 1 A. In the terminally differentiated villus cells, hensin was present exclusively in a basolateral pattern likely to represent extracellular localization, an identical distribution to that in permeabilized high density cells.

The epithelium of the prostate gland is another tissue that undergoes terminal differentiation in situ. Basal cells are sparsely located in the epithelium and they give rise to the luminal cells, which are terminally differentiated epithelial cells. Basal cells of the rodent prostate gland express cytokeratin7, whereas the luminal cells do not (Hayward et al., 1996a,b). As can be seen in Fig. 10 B, the rabbit basal cells also express cytokeratin7 (in green); these cells have a large number of vesicles that contain hensin (in red). On the other hand, in the luminal cells, hensin surrounds the cells in a pattern entirely similar to that of high density cells.

Discussion

There is increasing evidence that a number of polarized membrane proteins are targeted in a cell-type specific manner (for review see Al-Awqati et al., 1998). For instance, the human LDL receptor when expressed as a transgene in mice is located in the apical membrane of kidney epithelia but is basolateral in the intestine and liver (Pathak et al., 1990). The Na, K ATPase is basolateral in many epithelia, but is apical in the retinal pigment epithelium and choroid plexus (Gundersen et al., 1991). Most GPI-linked proteins are apical but they are basolateral in a thyroid cell line (Zurzolo et al., 1993). In the intercalated cell, we demonstrated that the same cell is capable of retargeting at least two proteins, the anion exchanger kAE1 and the H^+ ATPase to opposite membrane domains, but two other proteins, a basolateral glucose transporter and an apical lectin-binding protein did not change their polarized distribution (van Adelsberg et al., 1994).

These studies demonstrate that there does not appear to be a single class of mechanisms responsible for targeting polarized proteins in all cells. Because the protein that exhibits plastic polarity (e.g., Na, K ATPase or kAE1) is well polarized regardless of whether it is located in the apical or basolateral domain, one can conclude that each protein contains at least two potential targeting signals that are recognized differently by the cell machinery. Another version of this statement is that there may be a hierarchy of signals and that each cell reads these signals depending on its complement of targeting pathways. But remarkably, the cellular machinery that decodes these signals is also cell type specific. For instance, syntaxin 3, a t-SNARE critically involved in delivery of protein to the apical membrane of many epithelia (Low et al., 1996; Galli et al., 1998), is present in the basolateral membrane of the intercalated cell (Mandon et al., 1997). Furthermore, the pathway that vesicles take is also different: the apical targeting of dipeptidyl peptidaseIV is direct in some cells (MDCK), indirect in others (CaCO2; Hubbard et al., 1991), or exhibit both pathways in still others (LLC-PK1; Low et al., 1991). Recent observations showed that apical epithelial proteins when transfected into nonpolarized cells (fibroblasts) are localized in vesicles or membrane domains that are different from those that contain transfected basolateral proteins (Musch et al., 1996; Yoshimori et al., 1996). In summary, these studies demonstrate that there are multiple targeting pathways in many, even all cells. To generate a tissue-specific phenotype would probably require local factors that would provide additional information to the basic cellular targeting machinery or might even induce new pathways.

To begin to analyze these local factors, it is worth recalling that some of these plastic targeting events occur during

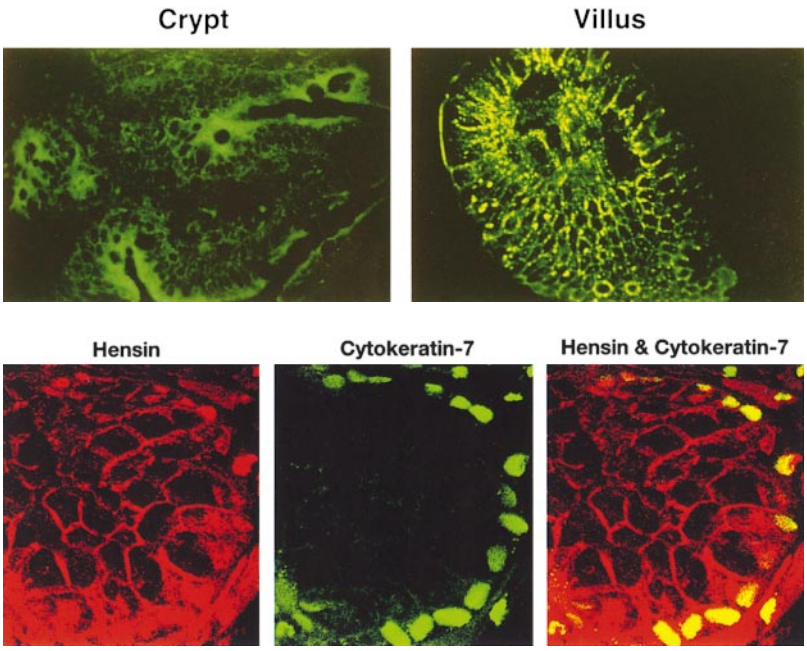

Figure 10. Distribution of hensin in small intestine and prostate gland. (Top) Rabbit small intestine was fixed, sectioned, and stained with anti-hensin antibodies. Confocal images of intestinal crypts (left) and villi (right) are shown. Note the staining pattern in crypts shows diffuse intracellular staining located mostly in the apical half of the cell. In villi, hensin is present in a basolateral pattern that surrounds the cell. (Bottom) Prostate glands: simultaneous staining with hensin (rhodamine) and cytokeratin7 (fluorescein). (Left) Red indicates the staining pattern of hensin in a typical prostate gland section. (Middle) shows the staining pattern of cytokeratin7, an exclusive marker of basal epithelia in rodent prostate in the same section. The right panel is the combined image.

development. The Na, K ATPase is found to be localized in the apical membrane in some nephrons during embryonic life and the probability of its basolateral location increases as the kidney matures (Avner et al., 1992). A membrane protein in the retinal pigment epithelium changes its polarized distribution during postnatal development (Marmorstein et al., 1996). Perhaps the signal for this reversal of polarity comes from a developmentally regulated extracellular instructive molecule. In the retinal pigment epithelium, the N-CAM molecule is apical in situ, but when the epithelium is dissociated from the neural retina and cultured in vitro N-CAM moves to the basolateral surface (Gundersen et al., 1993). Many developmental phenomena are mediated by factors that bind tightly to ECM proteins including: TGFβ family members, *wnt's*, and fibroblast growth factors. Further, ECM proteins that bind to these critical factors are themselves part of the developmental pathway and serve not only to generate gradients but also as reservoirs, activators, or inhibitors of these factors before they bind to their plasma membrane receptors. Our recent studies had demonstrated that one such protein, hensin, when deposited in the ECM of intercalated cells is sufficient to reverse the polarized distribution of the kidney form of band 3 (kAE1), and the proton ATPase (van Adelsberg et al., 1994; Takito et al., 1996). Hence, one hypothesis to emerge from this analysis is that tissue-specific proteins deposited in the ECM during development might instruct differentiating epithelia to target polarized proteins to one or another domain of the cell. If these ECM proteins are not present in that tissue, then the vesicle targeting pathway will come under the influence of other less dominant factors. To exhibit reversal of polarity, according to this formulation, the protein must contain multiple targeting sequences.

These speculations were solidified by the surprising finding of the present paper that hensin appeared to retarget several proteins and induce terminal differentiation in the intercalated cells. Both forms of the intercalated cells are stable when the two monolayers are confluent; all their cells are forming a true epithelial sheet, yet they exhibit different properties. Therefore, hensin must be acting as a binary switch to trigger the conversion of one phenotype to another, a process that is reminiscent of the induction of a differentiation program during development. Epithelial cells of the kidney (and many other organs) begin as mesenchymal cells that are induced to form the elementary epithelial phenotype, proto-epithelial cell. However, these cells only acquire a fully differentiated phenotype later in development. Terminally differentiated epithelia have several characteristics: (a) They contain a rich apical cytoskeletal network, the terminal web, which is composed of an actin mesh and specific cytokeratins. (b) Their apical membrane contains extensive specializations such as cilia, flagella, or brush-border microvilli. (c) They frequently contain vesicles or granules located in the apical half of the cell that are capable of fusion with the apical membrane in a manner regulated by cell calcium or other second messengers. (d) Their nuclei are present in the basal half of the cell. (e) They also assume a recognizable shape in simple epithelia, being columnar or cuboidal.

Remarkably, all of these characteristics were induced by hensin. The cells developed a terminal web of actin and cytokeratin19, their apical membranes formed an exuberant microvillar structure, and their shape became columnar. They even developed vesicles capable of regulated exocytosis. We had previously shown that the H^+ ATPase in the α-intercalated cell is packaged in vesicles that fuses with the apical membrane in response to an increase in the ambient pCO_2 acting to increase cell calcium (Gluck et al., 1982; Cannon et al., 1985). We suggest that hensin is the first protein in a new pathway for differentiation in these cell types. It had been known for some time that the ECM is critical for differentiation of epithelial cells. In fact, recent studies showed that fetal intestinal epithelia can start

to express terminally differentiated proteins such as villin and cytokeratin when cultured on matrigel, a complex ECM prepared from cancer cells (Sanderson et al., 1996). Hensin is expressed in a large number of epithelial tissues and at a high level in the intestine. Its distribution in intestinal crypt cells is similar to that of low density intercalated cells, whereas in villus cell it was similar to the terminally differentiated intercalated cell. We are presently investigating whether hensin is also involved in the differentiation of intestinal epithelia.

Hensin was accessible to its antibodies even when the high density cells were not permeabilized, and its distribution colocalized with collagen IV. How does the high density plating cause precipitation in the ECM? The localization of fibronectin fibrils in the ECM suggests a possible mechanism. Soluble fibronectin monomers cannot form fibrils unless their receptor, the integrin $\alpha_6\beta_1$ is activated (Wu et al., 1995). Once activated the receptor's affinity for fibronectin increases, allowing it to bind fibronectin and to form fibrils (Sechler et al., 1996). Perhaps high density seeding induces a change in the affinity of the hensin receptor that refolds hensin into an insoluble form. Alternatively, high density cells might secrete another protein that will cause precipitation of hensin in the extracellular space. We are presently investigating these two possibilities.

The role of the ECM in controlling cell shape is well-established in many cell types including epithelia (Ingber et al., 1986). Many studies have identified a pathway mediated by binding of integrins to components of the ECM that leads to activation of a signaling pathway mediated largely by activation of FAK. This protein is critical for organization of the actin cytoskeleton and leads to formation of a complex of actin binding proteins such as paxillin, ezrin, and moesin. Cell shape, motility, and ruffle formation are thought to be direct consequences of these events. Most of this information has been obtained in fibroblasts or in blood cells and the role of focal adhesions in epithelia is not as well studied. We found no change in the distribution of paxillin and FAK during the transition from low density to high density phenotypes. However, it was clear that there were large changes in other cytoskeletal components. A dramatic reorganization of the apical cytoplasm occurred that was characterized by all of the following: induction of vigorous apical endocytosis; development of exuberant microvillar formation, the new subapical localization of actin, and the possible induction or at least increased concentration of villin and cytokeratin19 in the subapical cytoplasm. The basal actin cytoskeleton was also different in the two phenotypes. Low density cells had many "stress fibers" in the basal region similar to what is seen in nonepithelial cells whereas the actin network in high density cells appeared to be more diffuse. How a basolateral extracellular molecule induces these changes in cell shape and the changes in apical cytoplasm is unknown at present. Recent studies have suggested that mechanical stress, such as that following binding of ECM proteins to their receptors have profound effects on cell functions, including the induction of complex programs of differentiation (Chen et al., 1997; Chicurel et al., 1998). The cellular mechanisms by which hensin induces these events awaits the identification of its signal transduction pathway and preliminary evidence suggests that a basolateral integral membrane glycoprotein acquires tyrosine phosphorylation within a short time after seeding these cells at high but not at low density.

The deduced amino acid sequence of hensin shows that it is composed of three domains, SRCR, (complement subcomponents Clr/Cls, Lleg F, Bmp1) CUB, and (Zona Pellucida) ZP (Takito et al., 1996 and manuscript submitted for publication). SRCR domains are cysteine rich domains of unknown function found in a variety of proteins (Resnick et al., 1994). The CUB domain was first identified in tolloid, a protein that activates decapentaplegic (dpp, the *Drosophila* TGFβ homologue) and mutations in that domain prevent dpp activation (Bork and Beckmann, 1993; Childs et al., 1994). The ZP domain, present in ZP sperm receptor proteins, bears some similarity to another TGFβ-binding protein, the type III receptor (Bork and Sander, 1992). Although these results suggest that hensin might bind to TGFβ or one of its many mammalian homologues, there is no evidence for this at present. Three other cDNAs have been reported that are composed of SRCR, CUB, and ZP domains. These include: CRP-ductin, a cDNA overexpressed in mouse intestinal crypt cells (Cheng et al., 1996); ebnerin, a partial cDNA overexpressed in rat von Ebner's gland (Li and Snyder, 1995); and DMBT1, a large human sequence that resides in chromosome 10q25-26 is deleted in a substantial fraction of several malignant brain tumors such as gliomas and glioblastomas (Mollenhauer et al., 1997). This region has also been implicated in other epithelial cancers such as prostate cancer. Because these sequences were first identified in four different species and the presence of large number of proteins with one or more of these domains in each species, it was not possible to decide by simple sequence comparisons whether they represented a new gene family, or whether they were alternately spliced versions of the same gene. We cloned the mouse and rabbit genomic sequences of hensin and partial sequences of these two led to the conclusion that all four sequences are derived from the same gene (Takito, J., L. Yan, C. Hikita, S. Vijayakumar, D. Warburtar, and Q. Al-Awqati, manuscript submitted for publication). Hensin appears to be involved in terminal differentiation and it is well-known that interruption in terminal differentiation pathways often leads to cancer. These occurrences raise the intriguing possibility that hensin is a tumor suppressor.

We are grateful to Lee Cohen-Gould for the performance of scanning electron microscopy and Theresa Swayne for expert assistance in confocal microscopy.

This work was supported by National Institutes of Health (NIH) grants DK-20999 and DK-39532. The Columbia Confocal Facility is supported by NIH grants RR10506 and CA13696.

Received for publication 23 July 1998 and in revised form 25 January 1999.

References

Achtstaetter, T., M. Hatzfield, R.A. Quinlan, D.C. Parmelee, and W.W. Franke. 1986. Separation of cytokeratin polypeptides by gel electrophoretic and chromatographic techniques and their identification by immunoblotting. *Methods Enzymol.* 134:355–371.

Al-Awqati, Q., S. Vijayakumar, C. Hikita, J. Chen, and J. Takito. 1998. Phenotypic plasticity in the intercalated cell: The hensin pathway. *Am. J. Physiol.* 275:F183–F190.

Avner, E.D., W.E. Sweeney, Jr., and W.J. Nelson. 1992. Abnormal sodium pump distribution during renal tubulogenesis in congenital murine polycys-

tic kidney disease. *Proc. Natl. Acad. Sci. USA*. 89:7447–7451.
Bard, J. The epithelial repertoire. *In* Morphogenesis: The Cellular and Molecular Processes of Development Anatomy. Cambridge University Press, New York. 1992. 181–237.
Bork, P., and C. Sander. 1992. A large domain common to sperm receptors (Zp2 and Zp3) and TGF-beta type III receptor. *FEBS (Fed. Eur. Biochem. Soc.) Lett.* 300:237–240.
Bork, P., and G. Beckmann. 1993. The CUB domain. A widespread module in developmentally regulated proteins. *J. Mol. Biol.* 231:539–545.
Cannon, C., J. van Adelsberg, S. Kelly, and Q. Al-Awqati. 1985. Carbon-dioxide-induced exocytotic insertions of H^+ pumps in turtle-bladder luminal membrane: role of cell pH and calcium. *Nature.* 314:443–446.
Chen, C.S., M. Mrkisch, S. Huang, G.M. Whitesides, and D.E. Ingber. 1997. Geometric control of cell life and death. *Science.* 276:1425–1428.
Chen, J., S. Vijayakumar, X. Li, and Q. Al-Awqati. 1998. Kanadaptin is a protein that interacts with the kidney but not the erythroid form of band 3. *J. Biol. Chem.* 273:1038–1043.
Cheng, H., M. Bjerknes, and H. Chen. 1996. CRP-ductin: a gene expressed in intestinal crypts and in pancreatic and hepatic ducts. *Anat. Rec.* 244:327–343.
Chicurel, M.E., C.S. Chen, and D.E. Ingber. 1998. Cellular control lies in the balance of forces. *Curr. Opin. Cell Biol.* 10:232–239.
Childs, S.R., and M.B. O'Connor. 1994. Two domains of the tolloid protein contribute to its unusual genetic interaction with decapentaplegic. *Dev. Biol.* 162:209–220.
Drubin, D.G., and W.J. Nelson. 1996. Origins of cell polarity. *Cell.* 84:335–344.
Eaton, S., and K. Simons. 1995. Apical, basal, and lateral cues for epithelial polarization. *Cell.* 82:5–8.
Edwards, J.C., J. van Adelsberg, M. Rater, D. Herzlinger, J. Lebowitz, and Q. Al-Awqati. 1992. Conditional immortalization of bicarbonate-secreting intercalated cells from rabbit. *Am. J. Physiol.* 263:C521–C529.
Friederich, E., C. Huet, M. Arpin, and D. Louvard. 1989. Villin induces microvilli growth and actin redistribution in transfected fibroblasts. *Cell.* 59: 461–475.
Galli, T., A. Zahraoui, V.V. Vaidyanathan, G. Raposo, J.M. Tian, M. Karin, H. Niemann, and D. Louvard. 1998. A novel tetanus neurotoxin-insensitive vesicle-associated membrane protein in SNARE complexes of the apical plasma membrane of epithelial cells. *Mol. Biol. Cell.* 9:1437–1448.
Gluck, S., C. Cannon, and Q. Al-Awqati. 1982. Exocytosis regulates urinary acidification in turtle bladder by rapid insertion of H^+ pumps into the luminal membrane. *Proc. Natl. Acad. Sci. USA*. 79:4327–4331.
Gundersen, D., J. Orlowski, and E. Rodriguez-Boulan. 1991. Apical polarity of Na, K-ATPase in retinal pigment epithelium is linked to a reversal of the ankyrin-fodrin submembrane cytoskeleton. *J. Cell Biol.* 112:863–872.
Gundersen, D., S.K. Powell, and E. Rodriguez-Boulan. 1993. Apical polarization of N-CAM in retinal pigment epithelium is dependent on contact with the neural retina. *J. Cell Biol.* 121:335–343.
Hagege, J., and G. Richet. 1970. Etude par microscopie electronique de la surface apicale des cellules de tube contourné distal du rein de rat. *C. R. Seances. Acad. Sci. D*. 271:331–332.
Hayward, S.W., L.S. Baskin, P.C. Haughney, A.R. Cunha, B.A. Foster, R. Dahiya, G.S. Prins, and G.R. Cunha. 1996a. Epithelial development in the rat ventral prostate, anterior prostate and seminal vesicle. *Acta Anat.* 155:81–93.
Hayward, S.W., J.R. Brody, and G.R. Cunha. 1996b. An edgewise look at basal epithelial cells: Three-dimensional views of the rat prostate, mammary gland and salivary gland. *Differentiation*. 60:219–227.
Hubbard, A.L. 1991. Targeting of membrane and secretory proteins to the apical domain in epithelial cells. *Semin. Cell Biol.* 2:365–374.
Ingber, D.E., J.A. Madri, and J.D. Jamieson. 1986. Basement membrane as a spatial organizer of polarized epithelia. Exogenous basement membrane reorients pancreatic epithelial tumor cells in vitro. *Am. J. Pathol.* 122:129–139.
LeFurgey, A., and C.C. Tisher. 1979. Morphology of the rabbit collecting duct. *Am. J. Anat.* 155:111–124.
Li, X.J., and S.H. Snyder. 1995. Molecular cloning of Ebnerin, a von Ebner's gland protein associated with taste buds. *J. Biol. Chem.* 270:17674–17679.
Louvard, D., M. Kedinger, and H.P. Hauri. 1992. The differentiating intestinal epithelial cell: Establishment and maintenance of functions through interactions between cellular structures. *Ann. Rev. Cell Biol.* 8:157–195.
Low, S.H., S.H. Wong, B.L. Tang, and W.J. Hong. 1991. Involvement of both vectorial and transcytotic pathways in the preferential apical cell surface localization of rat dipeptidyl peptidase IV in transfected LLC-PK1 cells. *J. Biol. Chem.* 266:19710–19716.
Low, S.H., S.J. Chapin, T. Weimbs, L.G. Komuves, M.K. Bennett, and K.E. Mostov. 1996. Differential localization of syntaxin isoforms in polarized Madin-Darby canine kidney cells. *Mol. Biol. Cell.* 7:2007–2018.
Mandon, B., S. Nielsen, B.K. Kishore, and M.A. Knepper. 1997. Expression of syntaxins in rat kidney. *Am. J. Physiol.* 273:F718–F730.
Marmorstein, A.D., V.L. Bonilha, S. Chiflet, J.M. Neill, and E. Rodriguez-Boulan. 1996. The polarity of the plasma membrane protein RET-PE2 in retinal pigment epithelium is developmentally regulated. *J. Cell. Sci.* 109:3025–3034.
Mollenhauer, J., S. Wiemann, W. Schurlen, B. Korn, Y. Hayashi, K.K. Wilgenbus, A.V. Deimling, and A. Poustka. 1997. DMBT1, a new member of the SRCR superfamily, on chromosome 10q25.3–26.1 is deleted in malignant brain tumours. *Nat. Genet.* 17:32–39.
Musch, A., H. Xu, D. Shields, and E. Rodriguez-Boulan. 1996. Transport of vesicular stomatitis virus G protein to the cell surface is signal mediated in polarized and nonpolarized cells. *J. Cell Biol.* 133:543–558.
Pathak, R.K., M. Yokodoe, R.E. Hammer, S.L. Hoffman, M.S. Brown, J.L. Goldstein, and R.G. Anderson. 1990. Tissue-specific sorting of the human LDL receptor in polarized epithelia of transgenic mice. *J. Cell Biol.* 111:347–359.
Resnick, D., A. Pearson, and M. Krieger. 1994. The SRCR superfamily: a family reminiscent of the Ig superfamily. *Trends Biochem. Sci.* 19:5–8.1994.
Salas, P.J., M.L. Rodriguez, A.L. Viciana, D.E. Vega-Salas, and H.P. Hauri. 1997. The apical submembrane cytoskeleton participates in the organization of the apical pole in epithelial cells. *J. Cell Biol.* 137:359–375.
Sanderson, I.R., R.M. Ezzell, M. Kedinger, M. Erlanger, Z.X. Xu, E. Pringault, S. Leon-Robine, D. Louvard, and W.A. Walker. 1996. Human fetal eneterocytes *in vitro*: Modulation of the phenotype by extracellular matrix. *Proc. Natl. Acad. Sci. USA*. 93:7717–7722.
Schuster, V.L. 1993. Function and regulation of collecting duct intercalated cells. *Annu. Rev. Physiol.* 55:267–288.
Schwartz, G.J., J. Barasch, and Q. Al-Awqati. 1985. Plasticity of functional epithelial polarity. *Nature.* 318:368–371.
Sechler, J.L., Y. Takada, and J.E. Schwarzbauer. 1996. Altered rate of fibronectin matrix assembly by deletion of the first type III repeats. *J. Cell Biol.* 134: 573–583.
Simon, T.C., and J.I. Gordon. 1995. Intestinal epithelial cell differentiation: new insights from mice, flies, and nematodes. *Curr. Opin. Genet. Dev*. 5:577–586.
Stasiak, C.P., P.E. Purkis, I.M. Leigh, and E.B. Lane. 1989. Keratin 19: predicted amino acid sequence and broad tissue distribution suggest it evolved from keratinocyte keratins. *J. Invest. Dermatol.* 92:707–716.
Takito, J., C. Hikita, and Q. Al-Awqati. 1996. Hensin, a new collecting duct protein involved in the in vitro plasticity of intercalated cell polarity. *J. Clin. Invest.* 98:2325–2331.
van Adelsberg, J.S., J.C. Edwards, and Q. Al-Awqati. 1993. The apical Cl/HCO_3^- exchanger of β intercalated cells. *J. Biol. Chem*. 268:11283–11289.
van Adelsberg, J., J.C. Edwards, J. Takito, B. Kiss, and Q. Al-Awqati. 1994. An induced extracellular matrix protein reverses the polarity of band 3 in intercalated epithelial cells. *Cell.* 76:1053–1061.
van't Hof, W., A. Malik, S. Vijayakumar, J.Z. Qiao, J. van Adelsberg, and Q. Al-Awqati. 1997. The effect of apical and basolateral lipids on the function of the band 3 anion exchange protein. *J. Cell Biol.* 139:941–949.
Wu, C., V.M. Keivens, T.E. O'Toole, J.A. McDonald, and M.H. Ginsberg. 1995. Integrin activation and cytoskeletal interaction are essential for the assembly of a fibronectin matrix. *Cell.* 83:715–724.
Yoshimori, T., P. Keller, M.G. Roth, and K. Simons. 1996. Different biosynthetic transport routes to the plasma membrane in BHK and CHO cells. *J. Cell Biol.* 133:247–256.
Zurzolo, C., M.P. Lisanti, I.P. Caras, L. Nitsch, and E. Rodriguez-Boulan. 1993. Glycophosphatidylinositol-anchored proteins are preferentially targeted to the basolateral surface in Fischer rat thyroid epithelial cells. *J. Cell Biol.* 121: 1031–1039.